

# Magnetic Sensitivity Depending on Cu-thickness of NiFe/Cu/NiFe/IrMn Spin Valve Device

Jong-Gu Choi<sup>1</sup>, Jin-Yong Lee<sup>1</sup>, Jae-Won Choi<sup>1</sup>, Tae-Soon Jang<sup>1</sup>, Do-Guwn Hwang<sup>1,2</sup>,  
Jang-Rho Rhee<sup>3</sup> and Sang-Suk Lee<sup>1,2\*</sup>

<sup>1</sup>Department of Eastern-Western Biomedical Engineering, Sangji University, Gangwon 220-702, Korea

<sup>2</sup>Department of Oriental Biomedical Engineering, Sangji University, Gangwon 220-702, Korea

<sup>3</sup>Department of Physics, Sookmyung Women's University, Seoul 140-742, Korea

## 1. Shape Magnetic Anisotropy on Magnetic Easy Axis of NiFe/Cu/NiFe/IrMn Spin Valve Thin Film

The GMR-SV (giant magnetoresistance-spin valve) device depending on the micro patterned features according to two easy directions of longitudinal and transversal axes has been studied. The GMR-SV multilayer structure was Ta(5 nm)/NiFe(8 nm)/Cu(2.3 nm)/NiFe(4 nm)/IrMn(5 nm)/Ta(2.5 nm). The applied anisotropy direction of the GMR-SV thin film was performed under the magnitude of 300 Oe using by permanent magnet during the deposition. The size of micro patterned device was a  $1 \times 18 \mu\text{m}^2$  after the photo lithography process. Fig. 1(a) shows real photograph of the GMR-SV devices with 2-probe electrodes of 66 number patterned by photo lithography. The GMR-SV multilayer structure was Ta(5 nm)/NiFe(8 nm)/Cu(2.3 nm)/NiFe(4 nm)/IrMn(5 nm)/Ta(2.5 nm). Fig. 1(b) shows real photograph of the GMR-SV devices with 2-probe electrodes of 16 number. Fig. 1(c) shows real photography of one GMR-SV device with a size of  $1.02 \mu\text{m} \times 18.37 \mu\text{m}$  before deposition 2-probe electrodes of Cr/Cu thin films. Fig. 1(d) shows real photograph of the GMR-SV device with 2-probe electrode. Here the marks of arrows are noticed the easy and hard axes with switching status in each other for the two cases. In the aspects of the shape magnetic anisotropy effect, there are two conditions of fabrication for GMR-SV device. Firstly, the direction of sensing current was perpendicular to the magnetic easy axis of the pinned NiFe/IrMn bilayer with the transversal direction of device. Secondly, the direction of shape magnetic anisotropy was same to the magnetic easy axis of the free NiFe layer with the longitudinal direction of device.

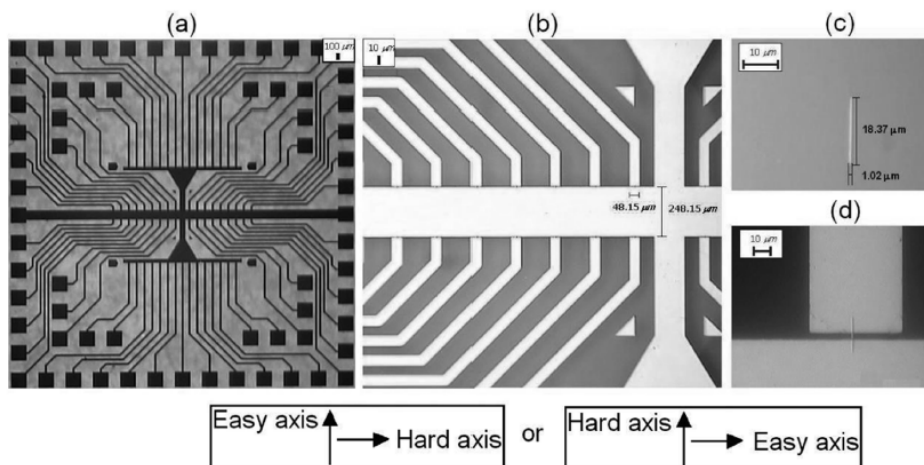


Fig. 1(a), 1(b), 1(c), and 1(d)

## 2. Magnetic Sensitivity Depending on Cu-thickness and Width and of IrMn Spin Valve Device

The Cu thickness dependence of magnetic sensitivity for the NiFe/Cu/NiFe/IrMn spin valve multilayer was investigated. Fig. 2(a) and (b) show major and minor MR curves of the Glass/Ta(5 nm)/NiFe(8 nm)/Cu(2.8 nm)/NiFe(4 nm)/IrMn(8 nm)/Ta(2.5 nm) GMR-SV film, respectively. Here are noted the definitions for surface resistance( $R_s$ ), maximum surface resistance( $R_m$ ), difference of surface resistance( $\Delta R$ ), magneoresistance ratio( $MR$ ), magnetic sensitivity( $MS$ ), raising coercivity( $H_1$ ), dropping coercivity( $H_2$ ), coercivity( $H_c$ ), and interlayer coupling field( $H_{int}$ ). The magnetic properties measured by minor MR(magneto-resistance) curves for the Ta(5 nm)/NiFe(8 nm)/Cu(3.5 nm)/NiFe(4 nm)/IrMn(8 nm)/Ta(2.5 nm) multilayer is  $MR = 1.46\%$ ,  $MS = 2.0\%/Oe$ ,  $H_c = 2.6 Oe$ , and  $H_{int} = 0.1 Oe$ . Table 1 shows Cu thickness dependence of magneto-resistance properties of free NiFe layer for the Glass/Ta(5 nm)/NiFe(8 nm)/Cu(t)/NiFe(4 nm)/IrMn(8 nm)/Ta(2.5 nm) films. Fig. 3(a) and (b) show minor MR curves for the GMR-SV device with a width of 9  $\mu m$  and thicknesses of Cu = 2.5 nm and Cu = 3.0 nm, respectively. Fig. 4(a) shows minor MR curve of the Ta(5 nm)/NiFe(8 nm)/Cu(3.5 nm)/NiFe(4 nm)/IrMn(8 nm)/Ta(2.5 nm) GMR-SV film ;  $MR = 1.46\%$ ,  $MS = 2.0\%/Oe$ ,  $H_c = 2.6 Oe$ , and  $H_{int} = 0.1 Oe$ . Fig. 4(b) shows minor  $MR$  curve for the GMR-SV device with a width of 1  $\mu m$  ;  $MR = 0.32\%$ ,  $MS = 0.3\%/Oe$ ,  $H_c = 0.1 Oe$ , and  $H_{int} = 0 Oe$ . Fig. 4(c) shows  $MS$  dependence as a function of width of GMR-SV device ;  $MS = 0.06\%/Oe \sim 0.3\%/Oe$ , width = 1  $\mu m \sim 10 \mu m$ . The magnetic sensitivities of GMR-SV devices with ten different widths and a same length of 4.45  $\mu m$  by fabricated by photo lithography decreased from 0.3  $\%/Oe$  to 0.06  $\%/Oe$  as from a width of 10  $\mu m$  to 1  $\mu m$ .

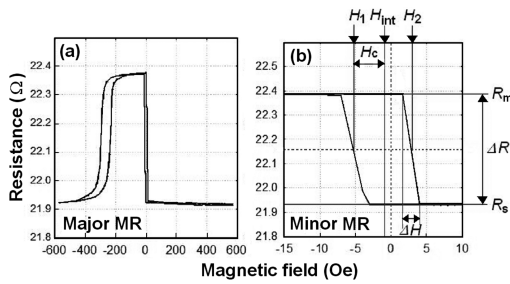


Fig. 2(a) and 2(b)

Table 1.

| Cu(t)<br>(nm) | $R_s$<br>[Ω] | $R_m$<br>[Ω] | $\Delta R$<br>[Ω] | MR<br>[%] | MS<br>[%/Oe] | $H_1$<br>[Oe] | $H_2$<br>[Oe] | $H_c$<br>[Oe] | $H_{int}$<br>[Oe] |
|---------------|--------------|--------------|-------------------|-----------|--------------|---------------|---------------|---------------|-------------------|
| 2.3           | 21.93        | 22.38        | 0.45              | 2.09      | 0.60         | -5.0          | +2.6          | 3.80          | -1.20             |
| 2.5           | 21.15        | 21.53        | 0.38              | 1.98      | 0.66         | -5.0          | +2.5          | 3.75          | -1.25             |
| 2.7           | 21.15        | 21.54        | 0.39              | 1.90      | 0.63         | -4.4          | +2.6          | 3.50          | -0.90             |
| 2.8           | 20.11        | 20.32        | 0.21              | 1.10      | 1.10         | -3.5          | +1.8          | 2.65          | -0.85             |
| 3.0           | 18.92        | 19.12        | 0.20              | 1.20      | 1.20         | -3.5          | +1.8          | 2.65          | -0.85             |
| 3.1           | 17.79        | 18.01        | 0.22              | 1.25      | 1.25         | -3.4          | +1.7          | 2.55          | -0.85             |
| 3.3           | 16.61        | 16.84        | 0.23              | 1.40      | 1.40         | -3.1          | +2.5          | 2.55          | -0.30             |
| 3.5           | 15.80        | 16.01        | 0.21              | 1.46      | 2.00         | -2.7          | +2.5          | 2.60          | -0.10             |
| 3.7           | 14.37        | 14.58        | 0.21              | 1.30      | 1.30         | -3.3          | +2.1          | 2.70          | -0.60             |

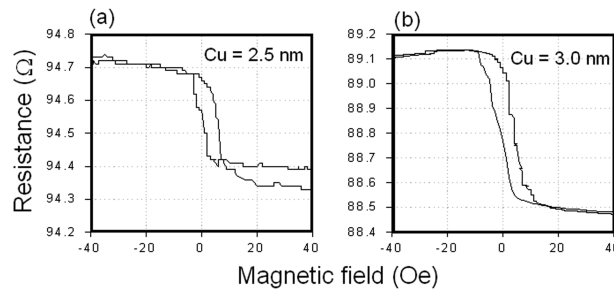


Fig. 3(a) and 3(b)

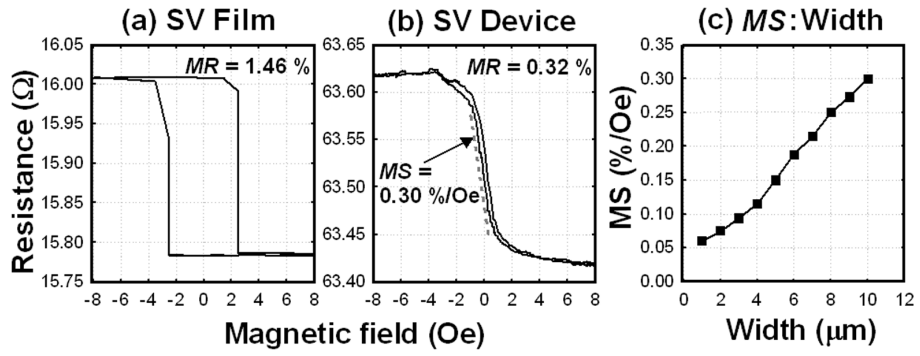


Fig. 4(a), 4(b), and 4(c)

## ACKNOWLEDGEMENT

This work was supported by the Research Program of Sangji University (2010).